JOURNAL OF AGRICULTURAL AND FOOD CHEMISTRY

Article

pubs.acs.org/JAFC

Transcriptome Analysis of Garlic-Induced Hepatoprotection against Alcoholic Fatty Liver

Rajasekaran Raghu,[†] Chun-Ting Liu,[†] Mong-Hsun Tsai,[‡] Xiaojia Tang,[§] Krishna R. Kalari,[§] Subbaya Subramanian,[⊥] and Lee-Yan Sheen*[,†]

[†]Institute of Food Science and Technology and [‡]Institute of Biotechnology, National Taiwan University, Taipei 106, Taiwan

[§]Division of Biostatistics and Informatics, Department of Health Sciences Research, Mayo Clinic, Rochester, Minnesota 55905, United States

[⊥]Department of Surgery, University of Minnesota, Minneapolis, Minnesota 55455, United States

ABSTRACT: Fatty liver induced by alcohol abuse is a major worldwide health hazard leading to morbidity and mortality. Previous studies indicate antifatty liver properties of garlic. This study investigated the molecular mechanisms of garlic oil (GO) or diallyl disulfide (DADS) imparted hepatoprotection against alcohol induced fatty liver in C57BL/6 mice using microarray-based global gene expression analysis. Alcohol liquid diet resulted in severe fatty liver with increased levels of serum aspartate aminotransferease and alanine aminotransferease as well as triglycerides and decreased levels of liver glutathione and antioxidant enzymes. The major canonical pathways implicated by alcohol treatment are the metabolisms of xenobiotics by cytochrome P450, glutathione, and arachidonic acid. Treatment with DADS or GO normalized the serum aminotransferease levels and liver antioxidant enzymes and reduced the contents of triglycerides and cholesterol. The canonical pathways involved in the amelioration of liver include arachidonic acid metabolism, altered T cell and B cell signaling, tryptophan metabolism, antigen presentation pathway for DADS, metabolism of xenobiotics, mitotic roles of Polo-like kinase, fatty acid metabolism, LPS/IL-1 mediated inhibition of RXR function, and C21-steroid hormone metabolism for GO.

KEYWORDS: *antifatty liver, diallyl disulfide, garlic oil, mechanism, transcriptome*

INTRODUCTION

Alcoholic liver disease (ALD) remains a notoriously significant health problem and is a major cause of morbidity and mortality worldwide.[1] Alcoholic fatty liver (AFL) is the initial stage wherein visible pathological symptoms appear in the liver subjected to alcohol abuse. On continued alcohol abuse, AFL (steatosis) develops to steatohepatitis, fibrosis, and cirrhosis, eventually leading to higher risks of hepatocelluar carcinoma. Because AFL is the precursor to a multitude of liver ailments, and is reversible if detected earlier, it is imperative to understand the underlying mechanisms of AFL. The molecular mechanism of AFL is slowly emerging at the level of gene transcription regulation, which is controlled through epigenetic mechanisms. However, most of the studies are based on tissue culture models.[2]

Garlic (*Allium sativum*) had been used for ages for various medicinal properties ranging from common colds to cancers.[3] The hepatoprotective property of garlic coupled with the hypocholesterolemic and hypolipidemic properties renders it a potential candidate for the treatment of ALD. Garlic also possesses antioxidant and anti-inflammatory properties, which render it a promising therapeutic intervention for ALD. Recent research has indicated the hepatoprotection of garlic extracts or their constituents on alcohol-[4−6] and non-alcohol-induced[7] fatty livers. However, the exact molecular mechanisms underlying this hepatoprotection are not fully understood.

Nutritional genomics or nutrigenomics identifies and understands mechanisms of molecular interaction between nutrients and/or other dietary bioactive compounds and the genome.[8] Microarray is one of the important technologies that find a promising application in nutrigenomics to provide new information, which can be used to ameliorate dietary regimens and to discover novel natural agents for the treatment of important diseases. In the present study, we investigated the hepatoprotective effects of garlic oil (GO) and its major organosulfur compound, diallyl disulfide (DADS), on alcohol-induced fatty liver in C57BL/6 mice. The molecular mechanisms involved in hepatoprotection are elucidated and compared by analyzing the global gene expression patterns using microarray. These results provide detailed insights into the pathways affected by the alcohol-induced fatty liver and the pathways effected by the constituents of garlic in restoring the fatty liver.

MATERIALS AND METHODS

Ethical Approval. This study strictly adheres to ethical guidelines on the care and use of laboratory animals issued by the National Taiwan University Institutional Animal Care and Use Committee (Approval No. NTU-IACUC-99-53).

Materials. GO was extracted as previously described.[9] Briefly, garlic obtained from a local market was peeled and crushed in 2 volumes of distilled water in a blender. The slurry was steam-distilled for 4 h, and the volatile compounds thus obtained were dehydrated and stored at −20 °C until use. The constituents of GO were analyzed by Thermo Scientific Focus GC equipped with an AI 3000 II autosampler, a flame ionization detector, and a Stabilwax (crossbond Carbowax-PEG)

Received: September 2, 2012
Revised: October 10, 2012
Accepted: October 11, 2012
Published: October 15, 2012

Restek column (60 m × 0.32 mm, 1.0 μm). The standards DAS (purity 97%) and DADS (purity > 79.0%) (Sigma-Aldrich) and DATS (purity > 95%) (ChromaDex) were used. The GO contained around 33% DADS and 30% DATS and traces of other volatiles. The diets for the mice consisted of Lieber−DeCarli liquid control diet (item 710027; Dyets Inc., Bethlehem, PA, USA) and Lieber−DeCarli EtOH liquid diet (item 710260; Dyets), and the compositions are given in Table 1.

Table 1. Formulation of Liquid Diet

ingredient	control diet (g/L)	ethanol diet (g/L)
casein (80 mesh)	41.40	41.40
DL-methionine	0.30	0.30
L-cystine	0.50	0.50
cellulose	10.00	10.00
maltose dextrin	115.20	25.60
corn oil	8.50	8.50
olive oil	28.4	28.40
safflower oil	2.70	2.70
mineral mix 210011[a]	8.75	8.75
vitamin mix 310011[b]	2.50	2.50
choline bitartarate	0.53	0.53
xanthan gum	3.00	3.00

[a]Mineral mix 210011 (g/kg): calcium carbonate, dibasic, 500.00; potassium citrate H_2O, 220; sodium chloride, 74.00; potassium sulfate, 52.00; magnesium oxide, 24.00; ferrous sulfate $7H_2O$, 4.95; zinc carbonate, 1.60; manganous sulfate H_2O, 4.60; cupric carbonate, 0.30; potassium iodate, 0.01; sodium slenite, 0.01; chromium potassium sulfate $12H_2O$, 0.55; sodium fluoride, 0.06; sucrose, 117.9. [b]Vitamin mix 310011 (per kg diet): thiamin HCl, 6.0 mg; riboflavin, 6.0 mg; pyrixodine HCl, 7 mg; niacin, 30 mg; calcium pantothenate, 16 mg; folic acid, 3 mg; biotin, 0.2 mg; cyanocobalamin (B12, 0.1%), 10 mg; menadione sodium bisulfate, 0.8 mg; vitamin E acetate, 24 IU; vitamin D3, 400 IU; inositol, 100 mg; *p*-aminobenzoic acid, 50 mg.

Animal Feeding and Experimental Design. Four-week-old male C57BL/6 mice purchased from BioLasco Co. (Taipei, Taiwan) were housed in individual cages under controlled temperature (25 ± 2 °C) and relative humidity (50%) with a 12 h light/12 h dark cycle at the Animal House Facility of Institute of Food Science and Technology. Twenty-four (24) mice were acclimated to tube feeding with Lieber−DeCarli liquid control diet over a 3 day period. To induce fatty liver, the diets of 18 mice were switched to Lieber−Decarli ethanol diet by gradually increasing the ethanol content from 1.34 to 6.7%. The mice were maintained under these two dietary regimensm, namely, the control (n = 6) and ethanol (n = 18). The control mice were pair-fed to the ethanol mice. The two diets are designed to be isocaloric at 1.0 kcal/mL with ethanol contributing about 36% of total calories.

On adaptation, the ethanol-fed mice were divided into three groups with six mice in each group and designated negative control, DADS, and GO groups. On the basis of the preliminary studies of our laboratory, mice were gavaged with GO (50 mg/kg bw) or DADS (15 mg/kg bw) mixed in 0.1 mL of olive oil. For the control and negative control groups, the same amount of olive oil (0.1 mL) was gavaged. Because DADS is the major organosulfur compound present in GO, DADS treatment was included in the present study. The mice were gavaged daily for 4 weeks. The mice were euthanized on the 29th day by CO_2. At sacrifice, blood was collected by cardiac puncture. Liver was collected and weighed. A portion of the liver was immersed in formalin for histopathological analysis, and the remaining liver was snap frozen in liquid nitrogen for RNA extraction and enzymatic analysis. Four samples (n = 4) from each treatment were selected for performing the microarray, real time qPCR, biochemical analysis, and histopathological examinations.

Serum Biochemical Analysis. Blood samples were left to sit for 1 h to allow the blood to coagulate. Serum was extracted by centrifuging at 12000 rpm for 5 min at 4 °C in a refrigerated centrifuge. The serum biochemical parameters of liver function indicators, such as aspartate aminotransferase (AST), alanine aminotransferase (ALT), triglyceride (TG), and cholesterol (TC), were estimated using commercial test strips (commercial ALT and AST Spotchem II reagent strips, Arkray Inc., Kyoto, Japan) using an automatic blood analyzer (Spotchem EZ).

Preparation of Liver Homogenate. Liver tissue (0.3 g) was homogenized in 10 volumes of ice-cold homogenization buffer (8 mM KH_2PO_4, 12 mM K_2HPO_4, and 1.5% KCl, pH 7.4) at 4 °C. The homogenate was then centrifuged at 10000 rpm for 30 min at 4 °C. The supernatant was stored at −80 °C and used to detect liver TG, TC, and hepatic antioxidant enzyme activity. The protein content in the liver homogenate was estimated spectrophotometrically by measuring the absorbance at 595 nm using the Bio-Rad protein assay kit (Hercules, CA, USA). Commercial kits procured from Cayman Chemical Co. (Ann Arbor, MI) were used to examine the hepatic antioxidant systems of glutathione (GSH) (item 703002), glutathione peroxidase (GPx) (item 703102), glutathione reductase (GRd) (item 703202), catalase (CAT) (item 707002), and superoxide dismutase (SOD) (item 706002).

Liver Biopsy Examination. Liver histological sections for pathological staining and semiquantitative analysis were made from the right lobe of liver to avoid observational bias. For histopathological observation, formalin-fixed paraffin-embedded (FFPE) liver sections were observed for the liver fatty accumulation, necrosis, fibrosis, and other changes in liver sections after staining with hematoxylin and eosin (H&E) and Sirius red. The pathological changes of liver, vacuolization, inflammation, and hepatic fibrosis were assigned scores by a pathologist.

Microarray. RNeasy MinElute Cleanup (Qiagen, GmbH) purified total RNA (600 ng) extracted from frozen liver tissue using TRIzol reagent (Invitrogen) was reverse transcribed into cRNA and biotin-UTP labeled using the Illumina TotalPrep RNA amplification kit (Ambion) after assessment of the RNA integrity number (RIN) by using an Agilent 2100 Bioanalyzer (Agilent Technologies, Palo Alto, CA, USA). The RIN was in the range of 8.3−9.8. cRNA (750 ng) was hybridized to the Illumina MouseRef-8 v2.0 Expression BeadChip using standard protocols (Illumina). Image data were converted into unnormalized sample probe profiles using Illumina GenomeStudio software v2010.1. All of the raw and processed microarray data have been deposited in NCBI's Gene Expression Omnibus[10] and are accessible through GEO Series accession no. GSE40334.

Microarray and Pathway Analysis. Raw intensity values were exported from GenomeStudio software for data processing and statistical computing in R (http://www.R-project.org) and Bioconductor (http://www.bioconductor.org). Microarray probes with detection p value of <0.05 were considered to be present in the analysis. Data quality of the probes was assessed using the Lumi − a Bioconductor package to process Illumina microarray data.[11] A robust spline normalization (RSN) method in the Lumi package that combines the features of the quantile and loess normalization methods was used for normalization of the data. The Limma − a Bioconductor R package was used to identify differentially expressed genes among groups.

Pathway analysis of the differentially expressed genes was carried out using Ingenuity Pathway Analysis (IPA) software. IPA constructs protein interactions based on a regularly updated knowledge database. The IPA knowledge database consists of millions of relationships between the molecules extracted from the biological literature and other databases. The IPA uses Fisher's exact test to determine significant pathways from an input gene list. The p value results in IPA software indicate the likelihood of the input gene list in a given pathway, found due to random chance.

Gene Ontology analysis was carried out with these identified transcripts in the database for Protein ANalysis THrough Evolutionary Relationships (PANTHER) to elucidate the molecular function, biological process, and PANTHER protein class (http://www.pantherdb.org/).[12]

Quantitative Real-Time Polymerase Chain Reaction (qRT-PCR). To validate the quantitative nature of the microarray expression

Table 2. qRT-PCR Primers Used for the Validation of Microarray Results

sl no.	gene	sequence	efficiency
1	GAPDH	sense, 5′-TGTGTCCGTCGTGGATCTGA-3′ antisense, 5′-CCTGCTTCACCACCTTCTTGAT-3′	1.02
2	Hsd3b4	sense, 5′-CACACCGCTGCTGCTATTG-3′ antisense, 5′-GTTGGCACACTGGCTTCC-3′	0.97
3	GSTP1	sense, 5′-CCATACACCATTGTCTACTTC-3′ antisense, 5′-TAACCACCTCCTCCTTCC-3′	1.00
4	PRC1	sense, 5′-ATTCAACCAACATCCAGTCC-3′ antisense, 5′-GTATCCGTCAGTCCAGTCC-3′	0.98
5	FMO3	sense, 5′-GCAATAGCACCACCATCC-3′ antisense, 5′-AACACTTCTACAGCCAACC-3′	0.96
6	CDKN1A	sense, 5′-AGGAGGAGCATGAATGGAGAC-3′ antisense, 5′-CGAAGAGACAACGGCACAC-3′	1.09

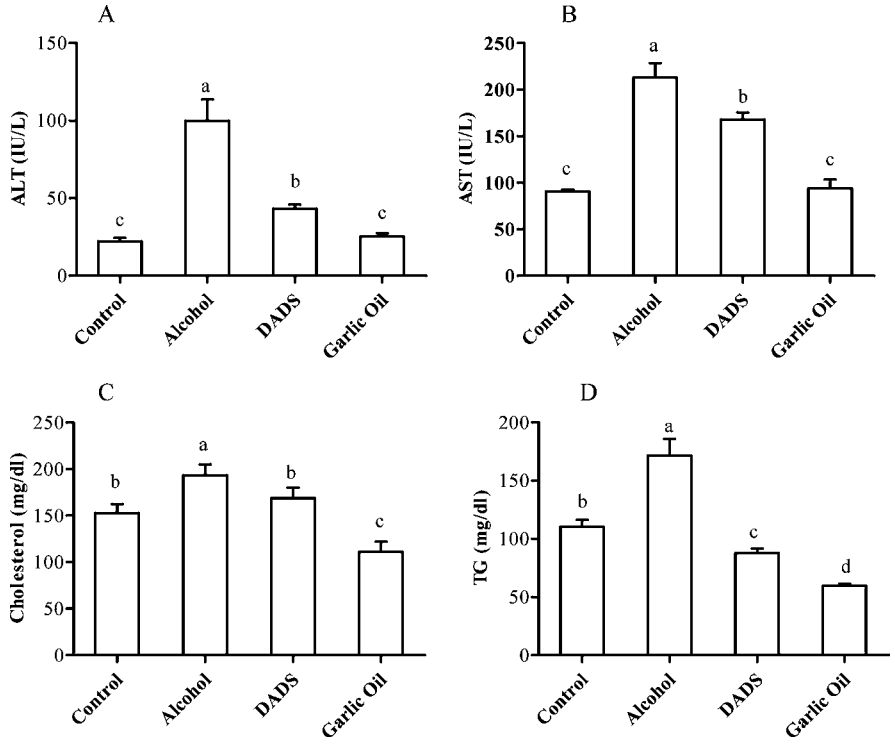

Figure 1. Effect of treatment of diallyl disulfide or garlic oil on serum (A) ALT, (B) AST, (C) cholesterol, and (D) triglycerides in chronic alcohol-induced fatty liver mice. Results are expressed as the mean ± SD (n = 4). Statistical analysis was performed using one-way analysis of variance (ANOVA) and Duncan's multiple-comparison test (SAS Institute Inc., Cary, NC, USA). Groups not sharing the same letter (a−d) are significantly different from one another ($p < 0.01$).

data, qRT-PCR was performed. First-strand cDNA was synthesized as a 40 μL reaction, with 2 μg of total RNA as the template using a QuantiTect reverse transcription kit (Qiagen, Hilden, Germany) according to the manufacturer's protocol. The qPCR primers (Table 2) were designed using Beacon Designer (Palo Alto, CA, USA, USA) and glyceraldehyde-3-phosphate dehydrogenase (GAPDH), which was used as endogenous control; the primer pair reported elsewhere[13] was used. Real-time PCR was performed on an ABI StepOne Plus Real-Time PCR System (Applied Biosystems, USA) using a KAPA SYBR FAST qPCR Kit Master Mix ABI Prism (KK4603, Kapa Biosystems). The qPCR reactions were performed with a final volume of 10 μL consisting of 1 μL of 25 times diluted first-strand cDNA, 1× qPCR master mix, and 200 nM of each forward and reverse primer. The PCR conditions were 95 °C for 1 min followed by 40 cycles of 95 °C for 3 s, 60 °C for 30 s, and, for verification of target gene amplifications, a dissociation stage at 95 °C for 15 s, 60 °C for 1 min, and 95 °C for 15 s. Gene expression was normalized to the endogenous control GAPDH. Normalized gene expression of alcohol, DADS, and GO groups was expressed relative to the control group. The expression levels were determined on four biological replicates, and each biological sample was replicated to obtain three technical replicates employing the $2^{-\Delta\Delta CT}$ method for gene expression.[14]

Statistical Analysis. Statistical analysis was performed using one-way analysis of variance (ANOVA) and Duncan's multiple-comparison test (SAS Institute Inc., Cary, NC, USA) to determine significant differences among means ($p < 0.01$).

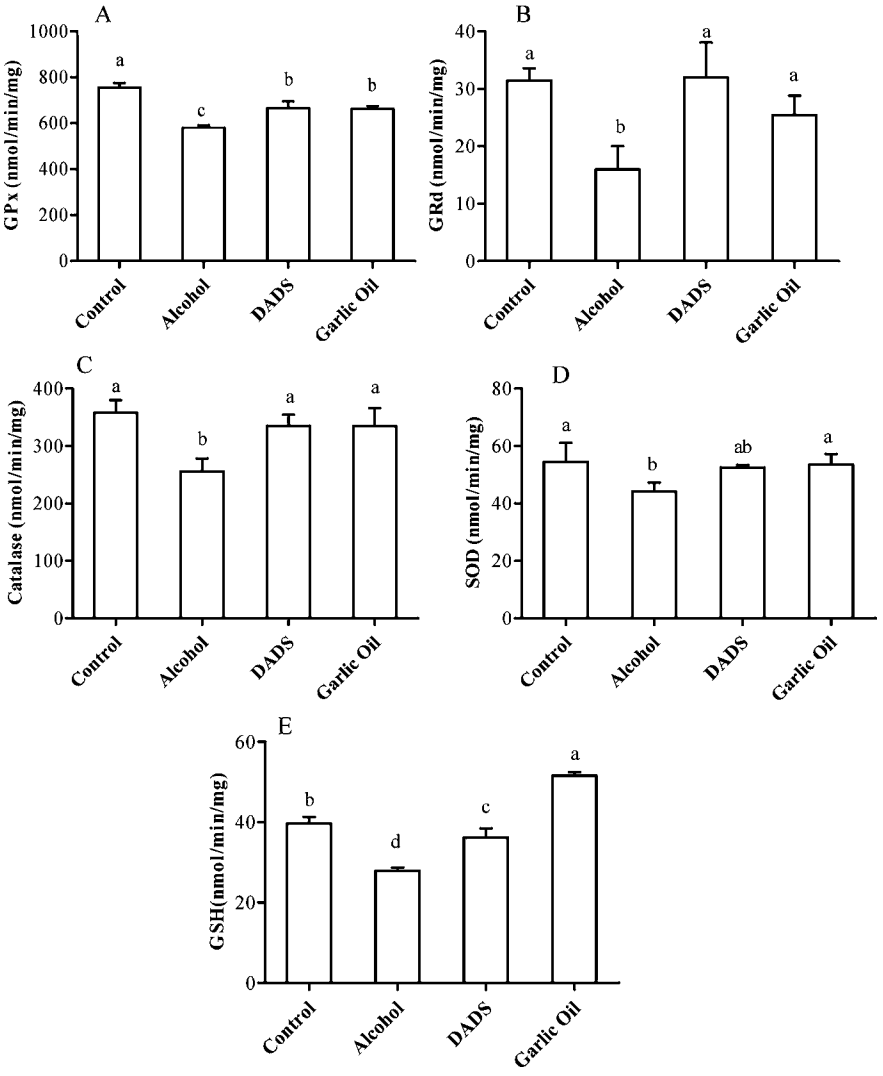

Figure 2. Effect of treatment of diallyl disulfide or garlic oil on hepatic (A) glutathione peroxidase, (B) glutathione reductase, (C) catalase, (D) superoxide dismutase, and (E) glutathione in liver of chronic alcohol-induced fatty liver mice. Results are expressed as the mean ± SD (n = 4). Statistical analysis was performed using one-way analysis of variance (ANOVA) and Duncan's multiple-comparison test (SAS Institute Inc.). Groups not sharing the same letter (a–c) are significantly different from one another ($p < 0.01$).

RESULTS

Biochemical Analysis. Serum AST and ALT levels of alcohol-fed mice significantly increased ($p < 0.01$) when compared to the control mice, recording a 4.5-fold increase in the serum ALT and a 2.3-fold increase in the AST. Chronic alcohol exposure significantly increased ($p < 0.01$) triglyceride content in serum and liver by 1.6- and 1.7-fold, respectively. A significant increase ($p < 0.01$) in serum cholesterol content was also observed in the alcohol group. Administration of DADS to the alcohol-fed mice reversed the harmful effects imparted by chronic alcohol exposure. A significant reduction ($p < 0.01$) in ALT and AST levels was recorded in the DADS group when compared to the alcohol group. A significant ($p < 0.01$) reduction of nearly 50% in the serum triglyceride content was recorded in the DADS group when compared to the alcohol group. Compared to the alcohol group, cholesterol content was also reduced significantly ($p < 0.01$) in the DADS group. A significant ($p < 0.01$) reduction in the levels of serum ALT, AST, cholesterol, and triglycerides was observed in the GO group when compared with the alcohol group (Figure 1).

Alcohol exposure for 28 days resulted in significant ($p < 0.01$) reduction in the activities of oxygen free radical scavenging enzymes such as GRd, GPx, CAT, and SOD when compared to the control liquid diet fed mice. Glutathione content in the liver decreased significantly ($p < 0.01$) due to chronic ethanol exposure when compared to the control. DADS-administered mice exhibited a significant ($p < 0.01$) increase in the hepatic antioxidant enzyme activities such as GRd, GPx, and CAT when compared with the alcohol group. In the GO group, enzyme activities of GRd, GPx, CAT, and SOD significantly ($p < 0.01$) increased when compared to the alcohol group, and these activities were comparable to the activities of the control group (Figure 2).

Feeding the alcohol liquid diet for 4 weeks induced fatty liver in C57BL/6 mice as evidenced by the histopathological sections, which recorded significantly ($p < 0.01$) pronounced severe/high fatty liver scores (Figure 3). The control group exhibited normal hepatic architecture, whereas the alcohol-fed mice indicated micro- and macrovesicles. There was significant ($p < 0.01$) restoration of the liver injury induced by alcohol as inferred from the fatty liver scores of 2.8 ± 0.8 for the DADS-fed group and 3.8 ± 0.4 for the GO-fed group.

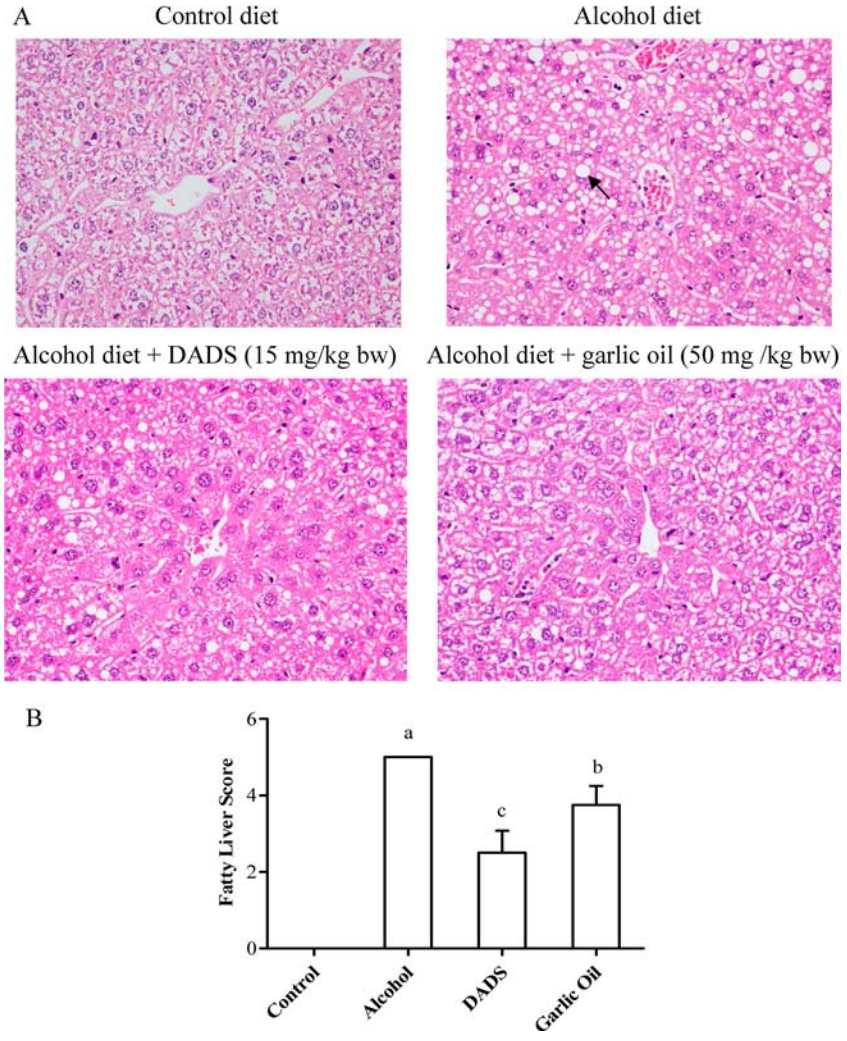

Figure 3. Histological features of representative liver sections stained with H&E (400×): (A) control sections show normal hepatic architecture (alcohol liquid diet induced severe fatty liver with micro- and macrovesicles (indicated by black arrow); DADS and GO groups indicate reduction in vesicles); (B) fatty liver score (results are expressed as the mean ± SD (n = 4); statistical analysis was performed using one-way analysis of variance (ANOVA) and Duncan's multiple-comparison test (SAS Institute Inc.); groups not sharing the same letter (a−c) are significantly different from one another (p < 0.01); degree of lesions was graded from one to five depending on severity: 1 = minimal (<1%); 2 = slight (1−25%); 3 = moderate (26−50%); 4 = moderate/severe (51−75%); 5 = severe/high (76−100%).

Transcriptome Analysis Fatty Liver with Garlic Constituents. The results of up-regulated and down-regulated genes and over-represented canonical pathways are given in Table 3. When control and chronic alcohol groups are compared, the top five up-regulated transcripts are cytochrome P450, family 2, subfamily b, polypeptide 9 (Cyp2b13/Cyp2b9); glutathione *S*-transferase α 5 (GSTA5); cytochrome P450, family 2, subfamily b, polypeptide 23 (Cyp2b23); kallikrein 1-related pepidase b4 (Klk1b1); and glutathione *S*-transferase, μ 3 (Gstm3); the prominent five down-regulated transcripts are cytochrome P450, family 7, subfamily A, polypeptide 1 (CYP7A1); TSC22 domain family, member 1 (TSC2D1); suppressor of cytokine signaling 2 (SOCS2); G0/G1switch 2 (G0S2); and hydroxy-Δ5-steroid dehydrogenase, 3β- and steroid δ-isomerase 4 (Hsd3b4).

To identify the differentially regulated transcripts in the DADS group, the alcohol group and DADS group were compared. The top five up-regulated genes were flavin-containing monooxygenase 3 (FMO3), cut-like homeobox 2 (CUX2), acyl-CoA thioesterase 1 (ACOT1), cytochrome P450, family 17, subfamily A, polypeptide 1 (CYP17A1), and suppressor of cytokine signaling 2 (SOCS2), and the prominent five down-regulated genes are hydroxy-Δ5-steroid dehydrogenase, 3 β- and steroid δ-isomerase 4 (Hsd3b4), kallikrein 1-related pepidase b4 (Klk1b1), ELOVL fatty acid elongase 3 (ELOVL3), serpin peptidase inhibitor, clade A (α-1 antiproteinase, antitrypsin), member 1 (SERPINA1), and major urinary protein 1 (Mup1).

GO (50 mg/kg bw) administration up-regulated parvalbumin (PVALB), flavin-containing monooxygenase 3 (FMO3), solute carrier family 4, anion exchanger, member 1 (erythrocyte membrane protein band 3, Diego blood group) (SLC4A1), cytochrome P450, family 17, subfamily A, polypeptide 1 (CY17A1), and aldehyde dehydrogenase 3 family, member A1 (ALDH3A1), whereas down-regulating the transcript levels of kallikrein 1-related pepidase b4 (KlKb1), PDZ binding kinase (PBK), protein regulator of cytokinesis 1 (PRC1), glutathione *S*-transferase α 5 (GSTA5), and serpin peptidase inhibitor, clade A (α-1 antiproteinase, antitrypsin), member 1 (SERPINA1).

The practical utility of performing global gene expression analysis is to identify the related pathways. The top five canonical

Table 3. Top Differentially Expressed Genes, Over-represented Canonical Pathways, and Enrichment Analysis on Microarray Data Set by DADS and Garlic Oil Administration

control vs alcohol	DADS vs alcohol	garlic oil vs alcohol
A. Top Five Up-regulated Genes (Fold Change)		
Cyp2b13/Cyp2b9 (6.60)	FMO3 (5.71)	PVALB (4.37)
GSTA5 (5.60)	CUX2 (2.90)	FMO3 (3.93)
Cyp2b23 (5.06)	ACOT1 (2.57)	SLC4A1 (2.87)
Klk1b1 (5.04)	CYP17A1 (2.55)	CYP17A1 (2.66)
Gstm3 (4.00)	SOCS2 (2.32)	ALDH3A1 (2.56)
B. Top Five Down-regulated Genes (Fold Change)		
CYP7A1 (−3.74)	Hsd3b4 (−5.41)	Klk1b1 (−4.72)
TSC22D1 (−3.17)	Klk1b1 (−5.03)	PBK (−2.35)
SOCS2 (−2.75)	ELOVL3 (−3.88)	PRC1 (−2.22)
G0S2 (−2.48)	SERPINA 1 (−2.96)	GSTA5 (−2.08)
Hsd3b4 (−2.30)	Mup1 (−2.49)	SERPINA 1 (−2.08)
C. Top Five Over-represented Ingenuity Canonical Pathways (−log (B−H *p* Value);[a]Ratio[b])		
metabolism of xenobiotics by cytochrome P450 (9.75E00; 1.61×10^{-1})	B cell development (2.37E00; 1.61×10^{-1}),	metabolism of xenobiotics by cytochrome P450 (1.56E00; 6.45×10^{-2})
glutathione metabolism (7.18E00; 2×10^{-1})	arachidonic acid metabolism (2.37E00; 7.34×10^{-2})	
arachidonic acid metabolism (4.98E00; 1.01×10^{-1})	altered T cell and B cell signaling in rheumatoid arthritis (2.37E00; 8.33×10^{-2})	mitotic roles of polo-like kinase (8.41×10^{-1}; 6.35×10^{-2})
aryl hydrocarbon receptor signaling (2.62E00; 6.47×10^{-2})	tryptophan metabolism (2.24E00; 6.72×10^{-2})	fatty acid metabolism (8.41×10^{-1}; 4.55×10^{-2})
LPS/IL-1-mediated inhibition of RXR fimction (2.62E00; 5.16×10^{-2})	antigen presentation pathway (1.94E00; 1.38×10^{-1})	LPS/IL-1 mediated inhibition of RXR function (4.6×10^{-1}; 2.82×10^{-2})
		C21-steroid hormone metabolism (4.51×10^{-1}; 1×10^{-1})

D. Enrichment Analysis (log 2 Ratio > 1.0 and p <0.05)

Entrez gene name (gene symbol)	control vs alcohol, fold change (p value)	DADS vs alcohol, fold change (p value)	garlic oil vs alcohol, fold change (p value)
both garlic oil and DADS			
kallikrein 1-related pepidase b4 (Klk1b1)	5.04 (2.41×10^{-2})	−5.03 (2.13×10^{-2})	−4.72 (3.14×10^{-2})
protein regulator of cytokinesis 1 (PRC1)	1.91 (2.33×10^{-4})	−1.63 (3.40×10^{-3})	−2.22 (9.98×10^{-5})
nucleolar and spindle associated protein 1 (NUSAP1)	1.42 (3.94×10^{-3})	−1.58 (3.33×10^{-3})	−1.48 (2.34×10^{-3})
RAP1 GTPase activating protein 2 (RAP1GAP2)	1.633 (9.69×10^{-3})	−1.623 (8.17×10^{-3})	−1.404 (1.67×10^{-2})
cell division cycle 20 homologue (*S. cerevisiae*) (CDC20)	1.06 (6.71×10^{-3})	−1.08 (9.55×10^{-3})	−1.36 (9.34×10^{-4})
regulator of G-protein signaling 1 (RGS1)	1.04 (8.40×10^{-4})	−1.40 (3.76×10^{-3})	−1.23 (2.73×10^{-3})
cytochrome P450, family 26, subfamily A, polypeptide 1 (CYP26A1)	3.03 (5.29×10^{-5})	−0.76 (1.93×10^{-2})	−1.23 (1.67×10^{-3})
endothelial cell-specific molecule 1 (ESM1)	1.42 (7.59×10^{-3})	−1.37 (2.18×10^{-2})	−1.17 (2.23×10^{-2})
RAB30, member RAS oncogene family (RAB30)	−1.99 (3.38×10^{-5})	1.15 (1.73×10^{-2})	1.17 (4.38×10^{-3})
flavin-containing monooxygenase 3 (FMO3)	−1.05 (8.44×10^{-3})	5.71 (8.43×10^{-7})	3.93 (2.45×10^{-5})
garlic oil only			
glutathione *S*-transferase α 5 (GSTA5)	5.60 (1.37×10^{-7})	0.34 (4.53×10^{-1})	−2.08 (5.10×10^{-4})
serum amyloid A2 (SAA2)	1.12 (1.56×10^{-4})	1.47 (7.35×10^{-1})	−2.05 (6.39×10^{-5})
cyclin B1 (Ccnb1/Gm5593)	1.90 (8.20×10^{-3})	−1.10 (9.71×10^{-2})	−1.84 (7.27×10^{-3})
asparagine synthetase (glutamine-hydrolyzing) (ASNS)	1.80 (1.38×10^{-2})	0.20 (6.06×10^{-1})	−1.55 (3.27×10^{-2})
glutathione *S*-transferase, μ 3 (Gstm3)	4.00 (4.78×10^{-7})	0.09 (8.48×10^{-1})	−1.39 (9.98×10^{-4})
TIMP metallopeptidase inhibitor 1 (TIMP1)	1.24 (1.33×10^{-2})	−0.64 (2.02×10^{-1})	−1.01 (3.20×10^{-2})
hydroxysteroid (17-β) dehydrogenase 6 homologue (mouse) (HSD17B6)	−1.25 (4.64×10^{-4})	0.03 (9.16×10^{-1})	1.27 (2.92×10^{-3})
DADS only			
collagen, type III, α 1 (COL3A1)	1.24 (8.65×10^{-4})	−1.08 (2.31×10^{-3})	−0.87 (1.94×10^{-2})
inhibitor of DNA binding 1, dominant negative helix−loop−helix protein (ID1)	−1.39 (4.64×10^{-3})	1.11 (1.44×10^{-3})	0.88 (1.50×10^{-2})
D site of albumin promoter (albumin D-box) binding protein (DBP)	−1.92 (2.93×10^{-6})	1.64 (9.45×10^{-3})	0.92 (2.50×10^{-2})
ubiquitin-like with PHD and ring finger domains 1 (UHRF1)	1.05 (3.50×10^{-2})	−1.46 (5.80×10^{-3})	−0.77 (1.17×10^{-1})
CD209b antigen (Cd209b)	1.20 (6.67×10^{-3})	−1.10 (9.24×10^{-3})	−0.77 (5.48×10^{-2})
anillin, actin binding protein (ANLN)	1.24 (2.73×10^{-3})	−1.15 (2.58×10^{-3})	−0.56 (1.16×10^{-1})
protein phosphatase 1, regulatory subunit 3B (PPP1R3B)	1.05 (1.12×10^{-2})	−1.06 (6.66×10^{-3})	−0.41 (2.77×10^{-1})
TSC22 domain family, member 3 (TSC22D3)	1.45 (1.69×10^{-3})	−1.44 (2.43×10^{-5})	−0.35 (2.42×10^{-1})
FXYD domain containing ion transport regulator 6 (FXYD6)	1.51 (1.93×10^{-2})	−1.34 (3.84×10^{-2})	−0.25 (5.49×10^{-1})
DNA-damage-inducible transcript 4 (DDIT4)	3.04 (4.45×10^{-4})	−2.18 (4.83×10^{-3})	−0.15 (8.33×10^{-1})
connective tissue growth factor (CTGF)	1.45 (6.02×10^{-3})	−1.37 (1.51×10^{-3})	−0.15 (7.99×10^{-1})

Table 3. continued

D. Enrichment Analysis (log 2 Ratio > 1.0 and p <0.05)			
Entrez gene name (gene symbol)	control vs alcohol, fold change (p value)	DADS vs alcohol, fold change (p value)	garlic oil vs alcohol, fold change (p value)
potassium channel, subfamily K, member 5 (KCNK5)	1.04 (1.14×10^{-2})	−1.18 (1.12×10^{-2})	−0.12 (8.22×10^{-1})
Src-like-adaptor (SLA)	1.14 (5.75×10^{-4})	−1.28 (5.29×10^{-3})	−0.07 (6.56×10^{-1})
cytochrome P450, family 7, subfamily A, polypeptide 1 (CYP7A1)	−3.74 (8.11×10^{-5})	2.19 (3.38×10^{-2})	−0.07 (5.65×10^{-1})
v-maf musculoaponeurotic fibrosarcoma oncogene homologue B (avian) (MAFB)	1.98 (2.91×10^{-3})	−1.89 (4.60×10^{-3})	0.001 (9.10×10^{-1})
growth arrest and DNA-damage-inducible, α (GADD45A)	−1.62 (4.38×10^{-3})	1.69 (6.65×10^{-4})	0.12 (6.01×10^{-1})
fibroblast growth factor 21(FGF21)	−1.998 (1.76×10^{-3})	1.966 (2.82×10^{-3})	0.24 (7.19×10^{-1})
cyclin-dependent kinase inhibitor 1A (p21, Cip1) (CDKN1A)	2.77 (4.77×10^{-5})	−1.78 (5.95×10^{-3})	0.33 (7.33×10^{-1})
proprotein convertase subtilisin/kexin type 4 (PCSK4)	−1.56 (2.09×10^{-5})	1.11 (1.64×10^{-2})	0.41 (1.03×10^{-1})
glucokinase (hexokinase 4) (GCK)	1.73 (1.46×10^{-5})	−1.28 (1.80×10^{-3})	0.49 (1.22×10^{-1})
ring finger protein 186 (RNF186)	−1.28 (1.73×10^{-3})	1.29 (1.48×10^{-3})	0.52 (1.62×10^{-1})
aquaporin 4 (AQP4)	−1.351 (4.84×10^{-3})	1.221 (1.36×10^{-2})	0.572 (7.27×10^{-2})
prolactin receptor (PRLR)	−1.11 (2.55×10^{-3})	1.42 (4.43×10^{-5})	0.63 (1.36×10^{-1})
acyl-CoA thioesterase 1 (ACOT1)	−1.76 (5.47×10^{-3})	2.57 (2.03×10^{-4})	0.81 (4.05×10^{-1})
suppressor of cytokine signaling 2 (SOCS2)	−2.75 (2.76×10^{-4})	2.32 (3.50×10^{-4})	0.87 (4.73×10^{-1})
lipin 1 (LPIN1)	2.88 (1.73×10^{-4})	−2.10 (2.46×10^{-3})	1.86 (4.30×10^{-5})

[a]B−H, Benjamini−Hochberg multiple testing corrected p value. [b]Ratio, the number of genes related to fatty liver that map to the pathway divided by the total number of genes that map to the canonical pathway.

pathways are metabolism of xenobioitics by cytochrome P450, glutathione metabolism, arachidonic acid metabolism, aryl hydrocarbon receptor signaling, and LPS/IL-mediated inhibition of RXR function. The top pathway implicated is the lipid metabolism. The top five canonical pathways influenced by DADS treatment were B cell development, arachidonic acid metabolism, alteration of T cells, and B cell signaling in rheumatoid arthiritis, tryptophan metabolism, and antigen presentation pathway. The top five canonical pathways implicated by GO feeding are metabolism of xenobiotics by cytochrome P450, mitotic roles of polo-like kinase, fatty acid metabolism, LPS/IL-1 mediated inhibition of RXR function, and C21-steroid hormone metabolism.

Enrichment Analysis and Network Analysis in Liver Tissues. To identify the perturbed transcripts that were reversed by administration of DADS or GO, the log ratio of data sets, namely, control versus alcohol, DADS versus alcohol, and GO versus alcohol, were compared. Significantly differentially regulated transcripts (log 2 ratio > 1.0; $p < 0.05$) among the data sets are represented in Table 3. We identified 43 such transcripts. Of these 43 transcripts, 36 transcript levels were significantly restored by DADS administration, 17 transcript levels were significantly restored by GO, and 10 transcripts levels were restored in both DADS and GO. To gain further insights into the molecular function, biological process, and protein class, these genes were queried in the PANTHER database, and the results are presented in Table 4.

The two most significant gene networks identified by DADS treatment are depicted in Figure 4. Top functions of these genes were related to (1) tissue morphology and hematological system development and (2) function, behavior, lipid metabolism, small molecule biochemistry, and vitamin and mineral metabolism. The differentially expressed genes pertaining to these two networks are given in Table 5. The two most significant gene networks identified by GO treatment are presented in Figure 5. Top functions of the networks were related to (1) lipid metabolism, molecular transport, and small molecule biochemistry and (2) cellular function and maintenance, small molecule biochemistry, and molecular transport. The fold changes of the differentially expressed genes are depicted in Table 6.

Validation of Microarray by qRT-PCR. The quantitative expression results from microarray were validated and confirmed by qRT-PCR (Figure 6). Five significantly differentially regulated genes with fold change of >1 ($p < 0.05$) were chosen. All five selected genes (Hsd3b4, GSTP1, PRC1, FMO3, and CDKN1A) showed similar expression patterns consistent with the microarray expression data. This indicates the reliability of the microarray data set.

DISCUSSION

Alcohol-induced fatty liver leads to higher risks of acquiring fibrosis, cirrhosis, and hepatocellular carcinoma. Despite this serious health concern, little progress has been achieved in the management of this disease.[15] Garlic, known for its lipid-lowering[16] and hepatoprotective[17] properties, is receiving much research focus against alcohol-induced fatty liver[4−6,18,19] recently. However, the exact comprehensive mechanisms are yet to be understood fully. Toward this, this global gene expression study was conceived to unravel the molecular mechanisms underlying DADS or GO amelioration of alcohol-induced fatty liver using a mouse model.

ALT is present only in liver, whereas AST is present in liver, cardiac muscle, skeletal muscle, kidney, brain, pancreas, lungs, leukocytes, and erythrocytes,[20] and these two serve as reliable markers for liver function. Chronic alcohol abuse results in hepatocyte damage, liver injury, and inflammation leading to increased permeability.[21] This may be the reason for the significant release of membrane-bound ALT and AST in the bloodstream of ethanol-fed mice compared to the control group.[22] Chronic alcohol diet increased the triglyceride level, and this may be attributed to the increased availability of acetyl-CoA, which serves as substrate for lipid biosynthesis and ATP generation.[23] Furthermore, the depleted levels of the primary defense hepatic free radical scavenging antioxidants enzymes such as SOD, CAT, GPx, GRd, and GSH in response to alcohol feeding indicate their action against oxidative stress. The depleted levels of these enzymes may be due to the scavenging of the toxic

Table 4. Molecular Function, Biological Process, and PANTHER Protein Class of Genes with Altered Expression by DADS or Garlic Oil Administration

gene symbol	Gene Ontology molecular function	Gene Ontology biological process	PANTHER protein class
both garlic oil and DADS			
RAP1GAP2	protein binding, small GTPase regulator activity	cell adhesion	G-protein modulator
ESM1	growth factor activity		growth factor
RAB30	GTPase activity, protein binding	intracellular protein transport, receptor-mediated endocytosis, intracellular signaling cascade,	small GTPase
PRC1	structural constituent of cytoskeleton, microtubule binding	mitosis, cytokinesis	nonmotor microtubule binding protein
CDC20	protein binding	cell cycle, proteolysis,	enzyme modulator
Klk1b1	serine-type peptidase activity	cell cycle, proteolysis, ectoderm development, nervous system development	serine protease
FMO3	oxidoreductase activity	respiratory electron transport chain, metabolic process	oxygenase
CYP26A1	oxidoreductase activity	respiratory electron transport chain, vitamin metabolic process, steroid metabolic process	oxygenase
RGS1	protein binding, small GTPase regulator activity	immune system process, G-protein coupled receptor protein signaling pathway, dorsal/ventral axis specification	G-protein modulator
garlic oil only			
SAA2	lipid transporter activity, transmembrane transporter activity	immune system process	transporter, apolipoprotein, defense/immunity protein
Gstm3	transferase activity	immune system process, response to toxin	transferase
ASNS	ligase activity	cellular amino acid biosynthetic process	ligase
TIMP1	protein binding, metalloendopeptidase inhibitor activity	proteolysis	metalloprotease inhibitor
Gstm3	transferase activity	immune system process, response to toxin	transferase
HSD17B6	oxidoreductase activity	visual perception, sensory perception, steroid metabolic process	dehydrogenase, reductase
DADS only			
DBP		transport	transfer/carrier protein
TSC22D3	transcription factor activity	regulation of transcription from RNA polymerase II promoter	transcription factor
MAFB	transcription factor activity	cell cycle, regulation of transcription from RNA polymerase II promoter, ectoderm development, nervous system development	transcription factor, nucleic acid binding
PCSK4	serine-type peptidase activity	transmembrane receptor protein serine/threonine kinase signaling pathway, cell-matrix adhesion, proteolysis, mesoderm development	serine protease
SLA	receptor binding	immune system process, transmembrane receptor protein tyrosine kinase signaling pathway, cellular defense response	transmembrane receptor regulatory/adaptor protein, signaling molecule
AQP4	transmembrane transporter activity	transport	transporter
COL3A1	extracellular matrix structural constituent	cell adhesion, cellular component morphogenesis	extracellular matrix structural protein
Cd209b	receptor activity	macrophage activation, cell adhesion, cellular defense response	receptor, defense/immunity protein, cell adhesion molecule
CYP7A1	oxidoreductase activity	respiratory electron transport chain, cholesterol metabolic process	oxygenase
GCK	protein kinase activity	phosphate metabolic process, protein amino acid phosphorylation	protein kinase
SOCS2	cytokine activity, kinase inhibitor activity, kinase regulator activity	protein targeting, transmembrane receptor protein tyrosine kinase signaling pathway, negative regulation of apoptosis, JAK-STAT cascade, cell−cell signaling, cytokine-mediated signaling pathway, negative regulation of apoptosis, mesoderm development, hemopoiesis, cellular glucose homeostasis	cytokine, kinase inhibitor
DBP	transcription factor activity	transcription from RNA polymerase II promoter	transcription factor, nucleic acid binding
DBP	oxidoreductase activity	steroid metabolic process	dehydrogenase, reductase

dx.doi.org/10.1021/jf303800p | J. Agric. Food Chem. 2012, 60, 11104−11119

Table 4. continued

gene symbol	Gene Ontology molecular function	Gene Ontology biological process	PANTHER protein class
PPP1R3B	protein binding, phosphatase regulator activity	glycogen metabolic process	phosphatase modulator
CDKN1A	protein binding, kinase inhibitor activity, kinase regulator activity	cell cycle	kinase inhibitor
LPIN1		lipid metabolic process	
ID1	transcription factor activity, transcription factor activity	regulation of transcription from RNA polymerase II promoter	transcription factor
UHRF1	transcription factor activity, transcription factor activity	nucleobase, nucleoside, nucleotide and nucleic acid transport, cell cycle, metabolic process,	zinc finger transcription factor
CTGF	growth factor activity	cell cycle, transmembrane receptor protein tyrosine kinase signaling pathway, cell−cell signaling, cell−matrix adhesion, cell motion, mesoderm development, angiogenesis	growth factor
GCK	carbohydrate kinase activity	glycolysis	carbohydrate kinase
GADD45A		immune system process, apoptosis, MAPKKK cascade, DNA repair, cell cycle, response to stress	
PRLR	receptor activity	cytokine-mediated signaling pathway, intracellular signaling cascade, mesoderm development, mammary gland development	receptor
FXYD6	ion channel activity	ion transport, signal transduction	ion channel
FGF21	growth factor activity	transmembrane receptor protein tyrosine kinase signaling pathway, MAPKKK cascade, cell−cell signaling, ectoderm development, nervous system development	growth factor

radicals. Inhibition of the antioxidant system may lead to the accumulation of H_2O_2 or products of its decomposition.[24] Whereas the conversion of superoxide anion into H_2O_2 is catalyzed by SOD, catalase scavenges H_2O_2 that has been generated by free radical or by SOD while removing the superoxide anions. GSTs, a family of isozymes, also play a crucial role in protecting the cells against ROS by catalyzing the conjugation of GSH to a variety of electrophilic compounds.[25,26] Ethanol or its metabolic products, especially the toxic aldehydes, negatively affect the multigene family of the GST, resulting in its reduction, which may be attributed to the ethanol hepatotoxicity.[27] Acetaldehyde promotes excess use and turnover of GSH, resulting in significant depletion,[28] and our results are in accordance with this finding. Our research findings also show depleted levels of SOD, CAT, GPx, GRd, and GSH, which are in unison with these earlier reports.

To elucidate the molecular mechanisms of garlic constituents' antifatty liver properties, a global gene expression study was performed using the liver tissues from the four experimental groups. The top canonical pathways influenced by alcohol administration compared to that of control were that of the metabolism of xenobiotics by cytochrome P450, glutathione metabolism, arachidonic acid metabolism, aryl hydrocarbon receptor signaling, and LPS/IL-1-mediated inhibition of RXR function. Alcohol insult has been linked to the multigene family of cytochromes P450.[29] Whereas the biochemical analysis indicated depletion in the reduced glutathione content of liver on alcohol treatment, gene expression analysis indicated up-regulation of glutathione *S*-transferases, constituents of phase II system of the xenobiotics metabolism and glutathione metabolism. Taken together, it can be inferred that the elevated transferase reactions might have depleted the liver glutathione reserves similar to the findings of a previous study.[29] Also, the arachidonic acid metabolism pathway was found to be disturbed as the ethanol-induced cytochrome P450 enzymes may have played a role as reported earlier.[30] Aryl hydrocarbon receptor (AhR), a ligand-activated transcription factor recognized as a regulator of the expression of xenobiotic-metabolizing enzymes,[31] was also disturbed. Another key pathway tightly interlinked with ethanol metabolism, LPS/IL-1-mediated inhibition of RXR, was also impaired. Acetaldehyde, a product of alcohol metabolism, directly or indirectly disturbs the redox balance, which influences the RXR/PPAR functions, resulting in impaired lipid metabolism, oxidative stress, and release of pro-inflammatory cytokines.[32] As expected, the top network implicated in the alcohol-fed mice was lipid metabolism, because liver plays a key role in lipid metabolism and transport. Chronic alcohol abuse induced fatty liver symptoms due to the accumulation of lipid droplets as evident from the histopathology results. All of these results indicate that feeding Leiber−DeCarli ethanol liquid diet for 4 weeks induced alcoholic fatty liver symptoms in the experimental model tested.

Lipid accumulation and oxidative stress play critical roles in alcohol-induced fatty liver disease. Garlic, known for its hypolipidemic property, is bestowed with abundant antioxidants, and its constituent active compounds were proven to induce phase I and phase II enzymes. Hence, garlic serves as a potential hepatoprotective candidate against alcohol. Recently, more research has been focused on herbal remedies in alcoholic liver diseases.[33] One prominent and most effective folk herbal medicine is garlic, which has evidenced therapeutic potential against cancer,[34,35] immunomodulation, atherosclerosis, sclerosis, and cardioprotective effect by lowering lipids. Also, it is well

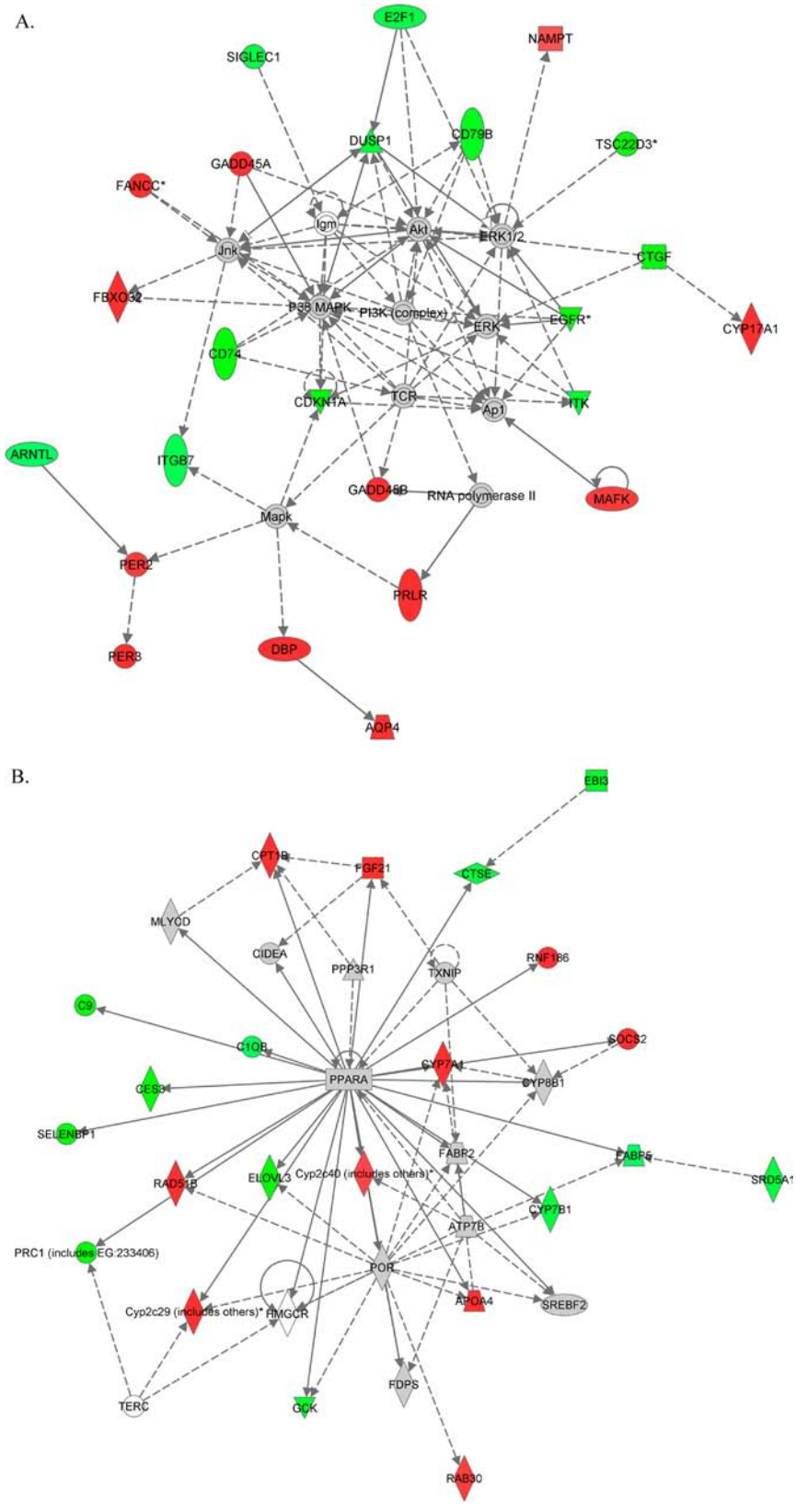

Figure 4. Biological networks identified by pathway analysis in response to DADS treatment. Intensity of node color indicates magnitude of up-regulation (red) or down-regulation (green): (A) network 1, related to tissue morphology, hematological system development and function, behavior; (B) network 2, lipid metabolism, small molecule biochemistry, vitamin and mineral metabolism. Solid arrow, induction and/or activation; dashed arrow, suppression and/or inhibition.

established that garlic imparts hepatoprotection, and recently there has been a great interest in employing garlic constituents such as GO[4] and aged black garlic[5] against alcohol-induced liver injury. In the present study we employed DADS and GO to

dx.doi.org/10.1021/jf303800p | J. Agric. Food Chem. 2012, 60, 11104−11119

Table 5. Top Two Biological Networks Identified by Pathway Analysis in Response to DADS Treatment

Entrez gene name (symbol)	fold change (p value)
Network 1. Tissue Morphology, Hematological System Development	
up-regulated genes	
cytochrome P450, family 17, subfamily A, polypeptide 1 (CYP17A1)	$2.55\ (6.19 \times 10^{-4})$
growth arrest and DNA-damage-inducible, α (GADD45A)	$1.69\ (6.65 \times 10^{-4})$
D site of albumin promoter (albumin D-box) binding protein (DBP)	$1.64\ (9.45 \times 10^{-3})$
growth arrest and DNA-damage-inducible, β (GADD45B)	$1.53\ (1.39 \times 10^{-2})$
prolactin receptor (PRLR)	$1.42\ (4.43 \times 10^{-5})$
period homologue 3 (*Drosophila*) (PER3)	$1.25\ (1.96 \times 10^{-3})$
F-box protein 32 (FBXO32)	$1.24\ (3.86 \times 10^{-3})$
Fanconi anemia, complementation group C (FANCC)	$1.23\ (4.48 \times 10^{-2})$
aquaporin 4 (AQP4)	$1.22\ (1.36 \times 10^{-2})$
v-maf musculoaponeurotic fibrosarcoma oncogene homologue K (avian) (MAFK)	$1.17\ (2.31 \times 10^{-3})$
period homologue 2 (*Drosophila*) (PER2)	$1.16\ (2.23 \times 10^{-2})$
nicotinamide phosphoribosyltransferase (NAMPT)	$1.02\ (1.86 \times 10^{-2})$
down-regulated genes	
cyclin-dependent kinase inhibitor 1A (p21, Cip1) (CDKN1A)	$-1.78\ (5.95 \times 10^{-3})$
CD74 molecule, major histocompatibility complex, class II invariant chain (CD74)	$-1.71\ (2.87 \times 10^{-4})$
TSC22 domain family, member 3 (TSC22D3)	$-1.44\ (2.43 \times 10^{-5})$
epidermal growth factor receptor (EGFR)	$-1.38\ (2.63 \times 10^{-3})$
connective tissue growth factor (CTGF)	$-1.37\ (1.51 \times 10^{-3})$
CD79b molecule, immunoglobulin-associated β (CD79B)	$-1.30\ (3.29 \times 10^{-3})$
IL2-inducible T-cell kinase (ITK)	$-1.24\ (2.10 \times 10^{-2})$
dual specificity phosphatase 1 (DUSP1)	$-1.21\ (6.57 \times 10^{-4})$
sialic acid binding Ig-like lectin 1, sialoadhesin (SIGLEC1)	$-1.16\ (8.69 \times 10^{-3})$
E2F transcription factor 1 (E2F1)	$-1.15\ (3.88 \times 10^{-4})$
integrin, β (ITGB7)	$-1.10\ (7.91 \times 10^{-3})$
aryl hydrocarbon receptor nuclear translocator-like (ARNTL)	$-1.02\ (1.24 \times 10^{-2})$
Network 2. Function, Behavior, Lipid Metabolism, Small Molecule Biochemistry, Vitamin and Mineral Metabolism	
up-regulated genes	
suppressor of cytokine signaling 2 (SOCS2)	$2.32\ (3.50 \times 10^{-4})$
cytochrome P450, family 7, subfamily A, polypeptide 1 (CYP7A1)	$2.19\ (3.38 \times 10^{-2})$
fibroblast growth factor 21 (FGF21)	$1.97\ (2.82 \times 10^{-3})$
apolipoprotein A-IV (APOA4)	$1.81\ (6.60 \times 10^{-5})$
cytochrome P450, family 2, subfamily c, polypeptide 29 (Cyp2C29)	$1.56\ (5.36 \times 10^{-4})$
ring finger protein 186 (RNF186)	$1.29\ (1.48 \times 10^{-3})$
RAD51 homologue B (*S. cerevisiae*) (RAD51B)	$1.29\ (8.55 \times 10^{-3})$
carnitine palmitoyltransferase 1B (muscle) (CPT1B)	$1.28\ (5.28 \times 10^{-3})$
member RAS oncogene family (RAB30)	$1.15\ (1.73 \times 10^{-2})$
cytochrome P450, family 2, subfamily c, polypeptide 40 (Cyp2c40)	$1.11\ (2.94 \times 10^{-2})$
down-regulated genes	
ELOVL fatty acid elongase 3(ELOVL3)	$-3.88\ (2.49 \times 10^{-4})$
carboxylesterase 3(CES3)	$-1.76\ (1.68 \times 10^{-5})$
selenium binding protein 1 (SELENBP1)	$-1.69\ (9.77 \times 10^{-3})$
protein regulator of cytokinesis 1 (PRC1)	$-1.63\ (3.40 \times 10^{-3})$
complement component 9 (C9)	$-1.46\ (3.27 \times 10^{-5})$
glucokinase (hexokinase 4) (GCK)	$-1.28\ (1.80 \times 10^{-3})$
Epstein–Barr virus induced 3 (EBI3)	$-1.27\ (5.04 \times 10^{-4})$
cathepsin E (CTSE)	$-1.19\ (6.14 \times 10^{-3})$
cytochrome P450, family 7, subfamily B, polypeptide 1 (CYP7B1)	$-1.18\ (1.74 \times 10^{-2})$
steroid-5-α-reductase, α polypeptide 1 (3-oxo-5α-steroid δ 4-dehydrogenase α 1) (SRD5A1)	$-1.18\ (2.56 \times 10^{-3})$
complement component 1, q subcomponent, B chain (C1QB)	$-1.04\ (9.11 \times 10^{-3})$
fatty acid binding protein 5 (psoriasis-associated) (FABP5)	$-1.02\ (4.12 \times 10^{-2})$

evaluate the hepatoprotective property against alcohol-induced fatty liver disease. The reliable biomarkers of liver, ALT and AST levels, reverted to near control levels in response to DADS or GO treatment. Similarly, the primary defense antioxidant levels and fatty liver also reverted to levels comparable to those of the control groups. Taken together, these results substantiate that DADS or GO imparts liver protection against alcohol injury.

Perturbations in global gene expression coupled with the pathway prediction tools pave the way to identify the underlying mechanistic pathways. The over-represented canonical pathways by DADS administration are B cell development, arachidonic acid metabolism, altered T cell and B cell signaling, tryptophan metabolism, and antigen presentation pathway. Of the top five canonical pathways, four pathways are involved in the immune system, and it is well established that garlic possesses immunomodulatory properties. The genes mostly disturbed in B cell development, altered T cell and B cell signaling, and antigen presentation pathway are the major histocompatibility complex (MHC) class II molecules (HLA-DMA, HLA-DQA1, HLA-DRB1, and HLA-DQB1). MHC-II molecules mediate adaptive immunity and present antigenic peptides from exogenous and membrane proteins.[36] The plausible mechanism of this down-regulation of the MHC-II molecules may be attributed to the interleukin-10-induced down-regulation[37] leading to inhibition of T cell activation and proliferation, eventually reducing the production of inflammatory factors.[38] The exact mechanism for this down-regulation warrants further research. Similar inhibition of the MHC-II pathway in response to vaccine immunization was reported in zebra fish.[39] Another important pathway implicated is arachidonic acid metabolism, and our earlier studies had indicated the modulation of hepatic arachidonic acid metabolism[40] by DADS and GO. Arachidonic acid, a precursor of eicosanoids, probably modulates the eicosanoid-dependent regulatory pathway as evidenced by the down-regulation of prostaglandin I2 synthase (PTGIS). Another gene down-regulated in this pathway is glutathione peroxidase (GPX2). GPx activity from biochemical estimation indicated a decrease in the DADS group when compared to the control group. The microarray data are in accordance with the biochemical result. The tryptophan metabolism pathway was also found to be implicated by DADS treatment. In this pathway, apart from the transcriptional disturbances of the cytochrome P450 levels, there is down-regulation of interleukin 4 induced 1 (IL4I1) and aldehyde oxidase 3 (Aox3) and up-regulation of aldehyde dehydrogenase 3 family, member A1 (ALDH3A1). The anti-inflammatory cytokine cascade activated by liver injury is repressed by DADS treatment. Whereas Aox3, a complex molybdoflavoprotein is down-regulated, ALDH3A1, which oxidizes aldehydes to acids and is mainly involved in detoxification of acetaldehyde derived from ethanol and lipid peroxidation, was up-regulated. Chronic alcohol abuse leads to the accumulation of acetaldehyde, which is metabolized to acetic acid by the aldehyde dehydrogenase, and

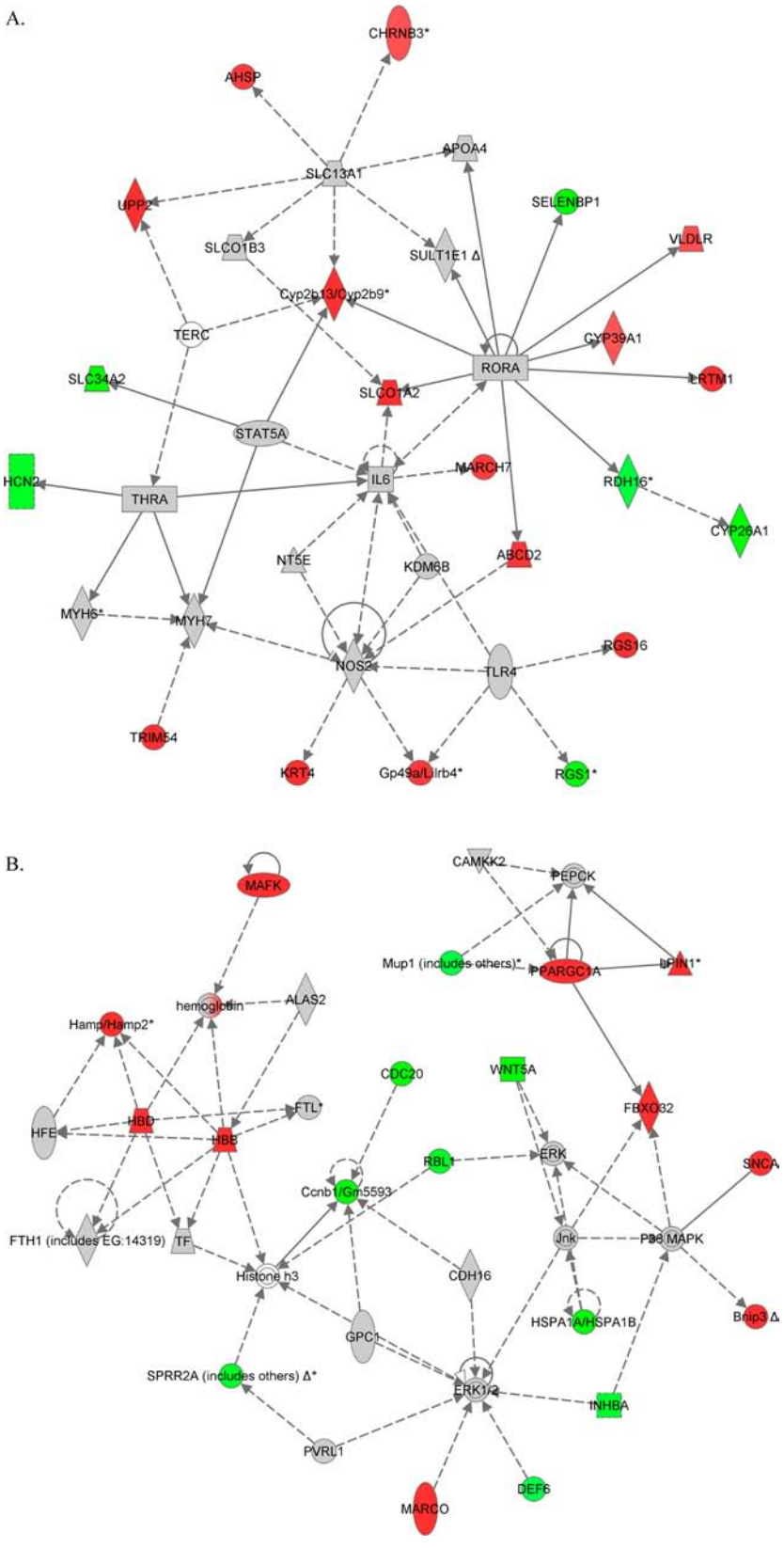

Figure 5. Biological networks identified by pathway analysis in response to garlic oil treatment. Intensity of node color indicates magnitude of up-regulation (red) or down-regulation (green): (A) network 1, related to lipid metabolism, molecular transport, small molecule biochemistry; (B) network 2, related to cellular function and maintenance, small molecule biochemistry, molecular transport. Solid arrow, induction and/or activation; dashed arrow, suppression and/or inhibition.

aged garlic extract protected mice from acetaldehyde toxicity.[41] In the present study, DADS feeding up-regulated ALDH3A1, and this may be one of the hepatoprotective mechanisms. Network analysis for DADS treatment revealed that the first identified

Table 6. Top Two Biological Networks Identified by Pathway Analysis in Response to Garlic Oil Treatment

Entrez gene name (symbol)	fold change (p value)
Network 1. Lipid Metabolism, Molecular Transport, Small Molecule Biochemistry	
up-regulated genes	
solute carrier organic anion transporter family, member 1A2 (SLCO1A2)	1.90 (9.23×10^{-6})
keratin 4 (KRT4)	1.90 (4.16×10^{-2})
regulator of G-protein signaling 16 (RGS16)	1.80 (3.75×10^{-3})
uridine phosphorylase 2 (UPP2)	1.65 (2.23×10^{-3})
leucine-rich repeats and transmembrane domains 1 (LRTM1)	1.57 (8.11×10^{-3})
cytochrome P450, family 2, subfamily b, polypeptide 9 (Cyp2b13/Cyp2b9)	1.46 (3.12×10^{-4})
tripartite motif containing 54 (TRIM54)	1.31 (5.77×10^{-3})
leukocyte immunoglobulin-like receptor, subfamily B, member 4 (Gp49a/Lilrb4)	1.16 (2.44×10^{-3})
alpha hemoglobin stabilizing protein (AHSP)	1.15 (4.30×10^{-3})
membrane-associated ring finger (C3HC4) 7 (MARCH7)	1.14 (3.13×10^{-3})
very low density lipoprotein receptor (VLDLR)	1.05 (2.78×10^{-2})
cholinergic receptor, nicotinic, β 3 (CHRNB3)	1.03 (2.23×10^{-2})
cytochrome P450, family 39, subfamily A, polypeptide 1 (CYP39A1)	1.01 (1.22×10^{-2})
down-regulated genes	
solute carrier family 34 (sodium phosphate), member 2 (SLC34A2)	−1.50 (6.26×10^{-3})
selenium binding protein 1(SELENBP1)	−1.48 (2.30×10^{-2})
cytochrome P450, family 26, subfamily A, polypeptide 1 (CYP26A1)	−1.23 (1.67×10^{-3})
regulator of G-protein signaling 1 (RGS1)	−1.23 (2.73×10^{-3})
hyperpolarization activated cyclic nucleotide-gated potassium channel 2 (HCN2)	−1.16 (3.79×10^{-3})
retinol dehydrogenase 16 (*all-trans*) (RDH16)	−1.05 (3.92×10^{-4})
Network 2. Cellular Function and Maintenance, Small Molecule Biochemistry, Molecular Transport	
up-regulated genes	
hemoglobin, δ (HBD)	2.04 (5.04×10^{-5})
lipin 1 (LPIN1)	1.86 (4.30×10^{-5})
synuclein, α (non A4 component of amyloid precursor) (SNCA)	1.77 (1.19×10^{-6})
v-maf musculoaponeurotic fibrosarcoma oncogene homologue K (avian) (MAFK)	1.61 (5.91×10^{-4})
hemoglobin, β (HBB)	1.58 (5.77×10^{-5})
F-box protein 32 (FBXO32)	1.40 (2.13×10^{-4})
hepcidin antimicrobial peptide (Hamp/Hamp2)	1.29 (2.37×10^{-3})
BCL2/adenovirus E1B interacting protein 3 (Bnip3)	1.25 (7.74×10^{-5})
peroxisome proliferator-activated receptor γ, coactivator 1 α (PPARGC1A)	1.22 (4.04×10^{-3})
down-regulated genes	
cyclin B1 (Ccnb1/Gm5593)	−1.84 (7.27×10^{-3})
heat shock 70 kDa protein 1A (HSPA1A/HSPA1B)	−1.42 (1.76×10^{-2})
cell division cycle 20 homologue (*S. cerevisiae*) (CDC20)	−1.36 (9.34×10^{-4})
wingless-type MMTV integration site family, member 5A (WNT5A)	−1.26 (6.99×10^{-4})
retinoblastoma-like 1 (p107) (RBL1)	−1.16 (2.26×10^{-3})
small proline-rich protein 2A (SPRR2A)	−1.14 (5.76×10^{-4})
inhibin, β A (INHBA)	−1.13 (2.47×10^{-4})
major urinary protein 1 (Mup1)	−1.04 (4.70×10^{-3})

network centered on P38 MAPK and ERK genes, whereas the second identified network centered on the PPARA gene.

Metabolism of xenobiotics by cytochrome P450, mitotic roles of polo-like kinase, fatty acid metabolism, LPS/IL-1-mediated inhibition of RXR function, and C21-steroid metabolism are the top five over-represented canonical pathways that are involved in the hepatoprotective property of GO. Mainly the cytochrome P450 transcript levels were influenced. It is interesting to note that some glutathione *S*-transferases (Gstm3, GSTA5) that were up-regulated in alcohol-exposed mice were down-regulated when GO was administered. This result corroborates the biochemical analysis data wherein liver glutathione reserves were restored by GO treatment. Because the glutathione reserves were restored, there might have been a reduction in the glutathione transferase activity. Also, the aldehyde dehydrogenease was found to be up-regulated in GO-administered mice as observed in DADS-administered mice.

Another canonical pathway implicated is the mitotic roles of polo-like kinase (Plk). Plk is a conserved serine/threonine kinase family that mediates G2/M transitions. Studies have shown that the inhibition of PLK1 activity causes mitotic arrest and eventually induces cancer cell apoptosis.[42] In the present study, GO administration down-regulated polo-like kinase 1 (PLK1), which in turn might have repressed cyclin B1 (Ccnb1/Gm5593). Also, cell division cycle 20 homologue (CDC20), which requires Plk phosphorylation, was down-regulated as indicated by the network analysis. Previously we have reported that DATS, a component of GO, induces apoptosis in human basal cell carcinoma cells.[34] Fatty liver subjects on continuous alcohol abuse developed hepatocelluar carcinoma. In the present study, the microarray data indicate GO treatment induced apoptosis in the liver.

LPS/IL-1-mediated inhibition of the retenoid X receptor (RXR) function pathway ranked fourth. RXR, a nuclear receptor, is suggested to play a key role in ethanol metabolism with its expression down-regulated by ethanol.[43] The transcripts FMO3, SLCO1A2, ALDH3A1, and PPARGC1A are up-regulated, whereas Gstm3 and GSTA5 are down-regulated. Activation of the hepatic stellate cells is a key step leading to fibrosis and cirrhosis in fatty liver progression, and PPARγ plays a key role in this activation.[44] Acetaldehyde, the oxidative product of ethanol, diffuses to adjacent cells, impairing their physiological activities. This acetaldehyde inactivates PPARγ by phosphorylation, and it is established that decrease in the PPARγ transcriptional activity results in increased synthesis of collagens.[45] In the present study, the up-regulation of ALDH3A1 might have triggered the acetaldehyde conversion to acetic acid. This reduction in acetaldehyde eventually might have inhibited the MAPK-mediated phosphorylation of PPARγ and hence up-regulated levels. PPARα expression was found to protect mice from high fat induced nonalcoholic fatty liver disease.[46] We can infer that GO treatment imparts protection against alcohol-induced fatty liver by influencing PPAR up-regulation. FMO3, an important player in detoxification,[47] was also up-regulated. Solute carrier organic anion transporter family, member 1A2 (SLCO1A2), was also up-regulated.

The C21-steroid hormone metabolism pathway was disturbed by GO treatment. The transcript level of cytochrome P450, family A, polypeptide 1 (CYP17A1) (responsible for 17,20-lyase and 17α-hydroxylase activities) and aldo-keto reductase family 1, member D1 (AKR1D1) are up-regulated. 3β-Hydroxy-Δ^5-steroid dehydrogenase-5 (Hsd3b5), a male-prevalent, testosterone-sensitive gene with hepatic expression, is negatively associated with steatosis.[48] Our qRT-PCR results corroborate this finding, exhibiting down-regulation of Hsd3b4 due to alcohol treatment, whereas the administration of either DADS or GO up-regulated Hsd3b4. Network analysis of the GO-treated samples indicated that the first network revolved around the IL

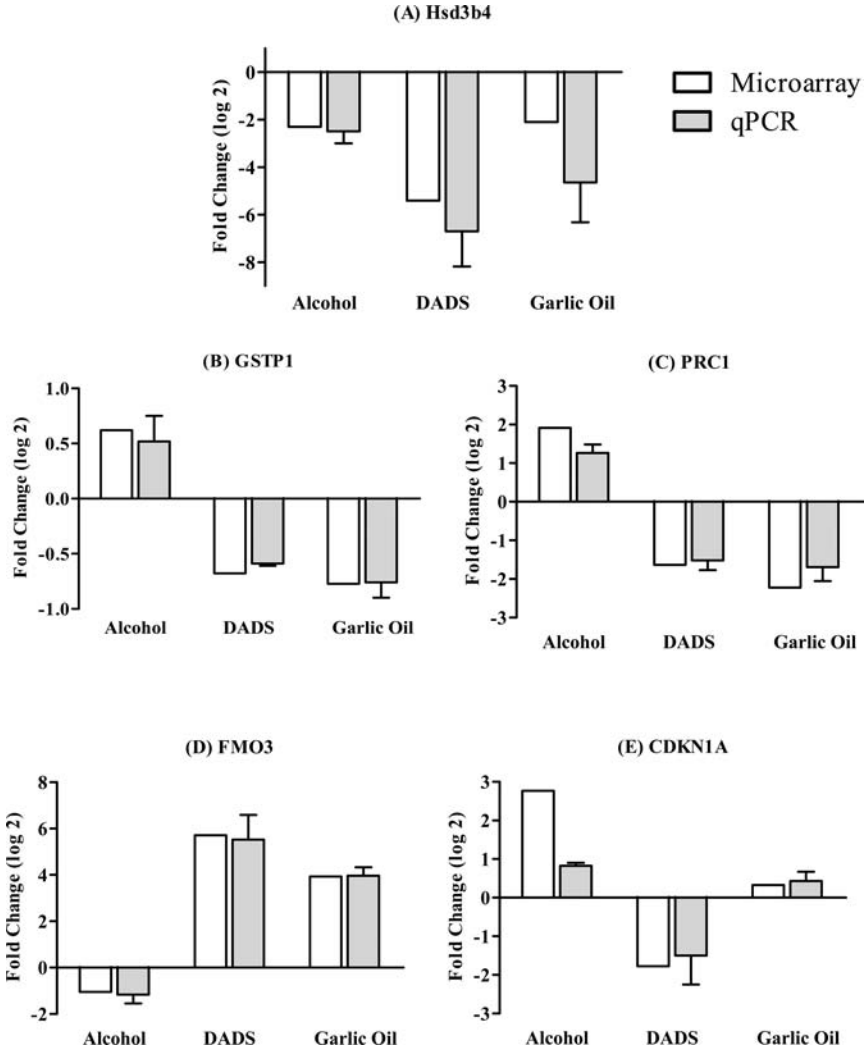

Figure 6. Validation of microarray gene expression results by RT-qPCR. Hepatic mRNA expression levels of (A) Hsd3b4, (B) GSTP1, (C) PRC1, (D) FMO3, and (E) CDKN1A were normalized to the endogenous control GAPDH. Normalized gene expression of alcohol, DADS, and garlic oil groups was expressed relative to control group.

6 gene, whereas the second network revolved around ERK1/2 genes.

One of the objectives of this study was to identify the genes impaired by alcohol feeding that were restored by DADS or GO. The majority of the transcripts that were significantly reverted in both DADS and GO groups are related to the cell cycle. Kallikrein 1-related peptidase b4 (Klk1b1), a secreted protein with immune or inflammatory function and a potential biomarker for certain cancers,[49] was up-regulated by alcohol feeding but down-regulated by either DADS or GO treatment. The transcripts significantly restored by GO treatment include the glutathione *S*-transferases (GSTA5 and Gstm3), serum amyloid A2 (SAA2), cyclin B1 (Ccnb1/Gm5593), asparagine synthetase (glutamine-hydrolyzing) (ASNS), TIMP metallopeptidase inhibitor 1 (TIMP1), and hydroxysteroid (17-β) dehydrogenase 6 homologue (HSD17B6). An isoform of serum amyloid A proteins, SAA2, up-regulated by alcohol treatment, was repressed by GO treatment and played a key role in inflammation and lipid metabolism. GO treatment repressed TIMP metallopeptidase inhibitor 1 (TIMP1), a glycoprotein with antiapoptotic function and a fibrogenesis marker. Recently, TIMP1 was found to be down-regulated by garlic extract in attenuating rat liver fibrosis.[50] Similarly, in the present study also the reduced TIMP1 may inhibit TGF-β1. Further in-depth studies at the protein level using knockout mice and employing immunohistochemical analyses would elucidate this subject more.

In conclusion, in the present study, a rodent model for alcohol-induced fatty liver was established. C57BL/6 mice fed Lieber−DeCarli ethanol liquid diet for 4 weeks developed fatty liver. DADS (15 mg/kg bw) and GO (50 mg/kg bw) imparted hepatoprotection to alcohol-induced fatty liver. A microarray-based approach was employed to elucidate the hepatoprotective mechanisms of garlic. The key pathways identified were related to the immune system, fatty acid metabolism, and cell cycle.

AUTHOR INFORMATION

Corresponding Author

*Postal address: No. 1, Section 4, Roosevelt Road, Taipei 106, Taiwan. Phone: 886-2-33664129. Fax: 886-2-23620849. E-mail: lysheen@ntu.edu.tw.

Funding

This research work was partially funded by the National Science Council of Taiwan under Grant NSC-99-2321-B-002-042.

Notes

The authors declare no competing financial interest.

■ ACKNOWLEDGMENTS

We thank Prof. Yi-Chen Lo for helpful discussions in real-time PCR.

■ REFERENCES

(1) Ramaiah, S.; Rivera, C.; Arteel, G. Early-phase alcoholic liver disease: an update on animal models, pathology, and pathogenesis. *Int. J. Toxicol.* **2004**, *23*, 217−231.

(2) French, S. W. In *Alcoholic Liver Disease Molecular Pathology of Liver Diseases*; Monga, S. P. S., Ed.; Springer: New York, 2011; Vol. *5*, pp 511−526.

(3) Wang, H. C.; Yang, J. H.; Hsieh, S. C.; Sheen, L. Y. Allyl sulfides inhibit cell growth of skin cancer cells through induction of DNA damage mediated G2/M arrest and apoptosis. *J. Agric. Food Chem.* **2010**, *58*, 7096−7103.

(4) Zeng, T.; Zhang, C. L.; Song, F. Y.; Zhao, X. L.; Xie, K. Q. Garlic oil alleviated ethanol-induced fat accumulation via modulation of SREBP-1, PPAR-α, and CYP2E1. *Food Chem. Toxicol.* **2012**, *50*, 485−491.

(5) Kim, M. H.; Kim, M. J.; Lee, J. H.; Han, J. I.; Kim, J. H.; Sok, D. E.; Kim, M. R. Hepatoprotective effect of aged black garlic on chronic alcohol-induced liver injury in rats. *J. Med. Food* **2011**, *14*, 732−738.

(6) Nencini, C.; Franchi, G. G.; Cavallo, F.; Micheli, L. Protective effect of *Allium neapolitanum* Cyr. versus *Allium sativum* L. on acute ethanol-induced oxidative stress in rat liver. *J. Med. Food* **2010**, *13*, 329−335.

(7) Xiao, J.; Ching, Y. P.; Liong, E. C.; Nanji, A. A.; Fung, M. L.; Tipoe, G. L. Garlic-derived *S*-allylmercaptocysteine is a hepato-protective agent in non-alcoholic fatty liver disease in vivo animal model. *Eur. J. Nutr.* **2012**, DOI: 10.1007/s00394-012-0301-0.

(8) Masotti, A.; Da Sacco, L.; Bottazzo, G. F.; Alisi, A. Microarray technology: a promising tool in nutrigenomics. *Crit. Rev. Food Sci. Nutr.* **2010**, *50*, 693−698.

(9) Sheen, L. Y.; Lin, S. Y.; Tsi, S. J. Odor assessments for volatile compounds of garlic and ginger essential oils by sniffing method of gas chromatography. *J. Chin. Agric. Chem. Soc.* **1992**, *30*, 14−24.

(10) Edgar, R.; Domrachev, M.; Lash, A. E. Gene Expression Omnibus: NCBI gene expression and hybridization array data repository. *Nucleic Acids Res.* **2002**, *30*, 207−210.

(11) Du, P.; Kibbe, W. A.; Lin, S. M. lumi: a pipeline for processing Illumina microarray. *Bioinformatics* **2008**, *24*, 1547−1548.

(12) Mi, H.; Dong, Q.; Muruganujan, A.; Gaudet, P.; Lewis, S.; Thomas, P. D. PANTHER version 7: improved phylogenetic trees, orthologs and collaboration with the Gene Ontology Consortium. *Nucleic Acids Res.* **2010**, *38*, D204−D210.

(13) Hirako, S.; Kim, H.-J.; Shimizu, S.; Chiba, H.; Matsumoto, A. Low-dose fish oil consumption prevents hepatic lipid accumulation in high cholesterol diet fed mice. *J. Agric. Food Chem.* **2011**, *59*, 13353−13359.

(14) Livak, K. J.; Schmittgen, T. D. Analysis of relative gene expression data using real-time quantitative PCR and the 2(−ΔΔC-(T)) method. *Methods* **2001**, *25*, 402−408.

(15) Gao, B.; Bataller, R. Alcoholic liver disease: pathogenesis and new therapeutic targets. *Gastroenterology* **2011**, *141*, 1572−1585.

(16) Augusti, K. T.; Mathew, P. T. Lipid lowering effect of allicin (diallyl disulphide-oxide) on long term feeding to normal rats. *Experientia* **1974**, *30*, 468−470.

(17) Kalantari, H.; Salehi, M. The protective effect of garlic oil on hepatotoxicity induced by acetaminophen in mice and comparison with N-acetylcysteine. *Saudi Med. J.* **2001**, *22*, 1080−1084.

(18) Shoetan, A.; Augusti, K. T.; Joseph, P. K. Hypolipidemic effects of garlic oil in rats fed ethanol and a high lipid diet. *Experientia* **1984**, *40*, 261−263.

(19) Bobboi, A.; Augusti, K. T.; Joseph, P. K. Hypolipidemic effects of onion oil and garlic oil in ethanol-fed rats. *Indian J. Biochem. Biophys.* **1984**, *21*, 211−213.

(20) Rej, R. Aspartate aminotransferase activity and isoenzyme proportions in human liver tissues. *Clin. Chem.* **1978**, *24*, 1971−1979.

(21) Goldberg, D. M.; Kapur, B. M. Enzymes and circulating proteins as markers of alcohol abuse. *Clin. Chim. Acta* **1994**, *226*, 191−209.

(22) Sillanaukee, P. Laboratory markers of alcohol abuse. *Alcohol Alcohol. (Oxford, U.K.)* **1996**, *31*, 613−616.

(23) Adamu, I.; Joseph, P. K.; Augusti, K. T. Hypolipidemic action of onion and garlic unsaturated oils in sucrose fed rats over a two-month period. *Experientia* **1982**, *38*, 899−901.

(24) Halliwell, B. Free radicals, antioxidants, and human disease: curiosity, cause, or consequence? *Lancet* **1994**, *344*, 721−724.

(25) Wilce, M. C.; Parker, M. W. Structure and function of glutathione *S*-transferases. *Biochim. Biophys. Acta* **1994**, *1205*, 1−18.

(26) Hayes, J. D.; Pulford, D. J. The glutathione *S*-transferase supergene family: regulation of GST and the contribution of the isoenzymes to cancer chemoprotection and drug resistance. *Crit. Rev. Biochem. Mol. Biol.* **1995**, *30*, 445−600.

(27) Alin, P.; Danielson, U. H.; Mannervik, B. 4-Hydroxyalk-2-enals are substrates for glutathione transferase. *FEBS Lett.* **1985**, *179*, 267−270.

(28) Lieber, C. S. Ethanol metabolism, cirrhosis and alcoholism. *Clin. Chim. Acta* **1997**, *257*, 59−84.

(29) Deaciuc, I. V.; Doherty, D. E.; Burikhanov, R.; Lee, E. Y.; Stromberg, A. J.; Peng, X.; de Villiers, W. J. Large-scale gene profiling of the liver in a mouse model of chronic, intragastric ethanol infusion. *J. Hepatol.* **2004**, *40*, 219−227.

(30) Nanji, A. A.; Zhao, S.; Lamb, R. G.; Sadrzadeh, S. M.; Dannenberg, A. J.; Waxman, D. J. Changes in microsomal phospholipases and arachidonic acid in experimental alcoholic liver injury: relationship to cytochrome P-450 2E1 induction and conjugated diene formation. *Alcohol.: Clin. Exp. Res.* **1993**, *17*, 598−603.

(31) Fujii-Kuriyama, Y.; Mimura, J. Molecular mechanisms of AhR functions in the regulation of cytochrome P450 genes. *Biochem. Biophys. Res. Commun.* **2005**, *338*, 311−317.

(32) Mello, T.; Polvani, S.; Galli, A. Peroxisome proliferator-activated receptor and retinoic x receptor in alcoholic liver disease. *PPAR Res.* **2009**, 748174.

(33) Lu, K. H.; Liu, C. T.; Raghu, R.; Sheen, L. Y. Therapeutic potential of Chinese herbal medicines in alcoholic liver disease. *J. Tradit. Complementary Med.* **2012**, *2*, 115−122.

(34) Wang, H. C.; Hsieh, S. C.; Yang, J. H.; Lin, S. Y.; Sheen, L. Y. Diallyl trisulfide induces apoptosis of human basal cell carcinoma cells via endoplasmic reticulum stress and the mitochondrial pathway. *Nutr. Cancer* **2012**, *64*, 770−780.

(35) Raghu, R.; Lu, K. H.; Sheen, L. Y. Recent research progress on garlic as a potential anticarcinogenic agent against major digestive cancers. *J. Tradit. Complementary Med.* **2012**, *2*, 192−201.

(36) Dengjel, J.; Schoor, O.; Fischer, R.; Reich, M.; Kraus, M.; Muller, M.; Kreymborg, K.; Altenberend, F.; Brandenburg, J.; Kalbacher, H.; Brock, R.; Driessen, C.; Rammensee, H. G.; Stevanovic, S. Autophagy promotes MHC class II presentation of peptides from intracellular source proteins. *Proc. Natl. Acad. Sci. U.S.A.* **2005**, *102*, 7922−7927.

(37) Huang, H. F.; Zeng, Z.; Chen, M. Q. Roles of Kupffer cells in liver transplantation. *Hepatogastroenterology* **2012**, *59*, 1251−1257.

(38) Mocellin, S.; Panelli, M. C.; Wang, E.; Nagorsen, D.; Marincola, F. M. The dual role of IL-10. *Trends Immunol.* **2003**, *24*, 36−43.

(39) Yang, D.; Liu, Q.; Yang, M.; Wu, H.; Wang, Q.; Xiao, J.; Zhang, Y. RNA-seq liver transcriptome analysis reveals an activated MHC-I pathway and an inhibited MHC-II pathway at the early stage of vaccine immunization in zebrafish. *BMC Genomics* **2012**, *13*, 319.

(40) Liu, C.-T.; Chen, H.-W.; Sheen, L.-Y.; Kung, Y.-L.; Chen, P. C.-H.; Lii, C.-K. Effect of garlic oil on hepatic arachidonic acid content and immune response in rats. *J. Agric. Food Chem.* **1998**, *46*, 4642−4647.

(41) Kasuga, S.; Uda, N.; Kyo, E.; Ushijima, M.; Morihara, N.; Itakura, Y. Pharmacologic activities of aged garlic extract in comparison with other garlic preparations. *J. Nutr.* **2001**, *131*, 1080S−1084S.
(42) Liu, X.; Choy, E.; Harmon, D.; Yang, S.; Yang, C.; Mankin, H.; Hornicek, F. J.; Duan, Z. Inhibition of polo-like kinase 1 leads to the suppression of osteosarcoma cell growth in vitro and in vivo. *Anticancer Drugs* **2011**, *22*, 444−453.
(43) Wan, Y. J.; Morimoto, M.; Thurman, R. G.; Bojes, H. K.; French, S. W. Expression of the peroxisome proliferator-activated receptor gene is decreased in experimental alcoholic liver disease. *Life Sci.* **1995**, *56*, 307−317.
(44) Galli, A.; Crabb, D.; Price, D.; Ceni, E.; Salzano, R.; Surrenti, C.; Casini, A. Peroxisome proliferator-activated receptor gamma transcriptional regulation is involved in platelet-derived growth factor-induced proliferation of human hepatic stellate cells. *Hepatology* **2000**, *31*, 101−108.
(45) Galli, A.; Crabb, D. W.; Ceni, E.; Salzano, R.; Mello, T.; Svegliati-Baroni, G.; Ridolfi, F.; Trozzi, L.; Surrenti, C.; Casini, A. Antidiabetic thiazolidinediones inhibit collagen synthesis and hepatic stellate cell activation in vivo and in vitro. *Gastroenterology* **2002**, *122*, 1924−1940.
(46) Abdelmegeed, M. A.; Yoo, S. H.; Henderson, L. E.; Gonzalez, F. J.; Woodcroft, K. J.; Song, B. J. PPARα expression protects male mice from high fat-induced nonalcoholic fatty liver. *J. Nutr.* **2011**, *141*, 603−610.
(47) Celius, T.; Roblin, S.; Harper, P. A.; Matthews, J.; Boutros, P. C.; Pohjanvirta, R.; Okey, A. B. Aryl hydrocarbon receptor-dependent induction of flavin-containing monooxygenase mRNAs in mouse liver. *Drug Metab. Dispos.* **2008**, *36*, 2499−2505.
(48) Guillen, N.; Navarro, M. A.; Arnal, C.; Noone, E.; Arbones-Mainar, J. M.; Acin, S.; Surra, J. C.; Muniesa, P.; Roche, H. M.; Osada, J. Microarray analysis of hepatic gene expression identifies new genes involved in steatotic liver. *Physiol. Genomics* **2009**, *37*, 187−198.
(49) Diamandis, E. P.; Okui, A.; Mitsui, S.; Luo, L. Y.; Soosaipillai, A.; Grass, L.; Nakamura, T.; Howarth, D. J.; Yamaguchi, N. Human kallikrein 11: a new biomarker of prostate and ovarian carcinoma. *Cancer Res.* **2002**, *62*, 295−300.
(50) D'Argenio, G.; Mazzone, G.; Ribecco, M. T.; Lembo, V.; Vitaglione, P.; Guarino, M.; Morisco, F.; Napolitano, M.; Fogliano, V.; Caporaso, N. Garlic extract attenuating rat liver fibrosis by inhibiting TGF-β1. *Clin. Nutr.* **2012**, DOI: 10.1016/j.clnu.2012.07.001.